Oncogene (2005) 24, 4477–4485

www.nature.com/onc

ORIGINAL PAPERS

Increased dosage of *Runx1/AML1* acts as a positive modulator of myeloid leukemogenesis in BXH2 mice

Masatoshi Yanagida[1,3,6], Motomi Osato[1,2,6], Namiko Yamashita[1,3], Huang Liqun[2], Bindya Jacob[1], Feng Wu[3], Xinmin Cao[1], Takuro Nakamura[4], Tomomasa Yokomizo[5], Satoru Takahashi[5], Masayuki Yamamoto[5], Katsuya Shigesada[3] and Yoshiaki Ito*[,1,2]

[1]*Institute of Molecular and Cell Biology, Singapore;* [2]*Oncology Research Institute, National University of Singapore, Singapore;* [3]*Institute for Virus Research, Kyoto University, Kyoto, Japan;* [4]*The Cancer Institute, Japanese Foundation for Cancer Research, Tokyo, Japan;* [5]*Institute of Basic Medical Science and Center for Tsukuba Advanced Research Alliance, University of Tsukuba, Ibaraki, Japan*

The *RUNX1/AML1* gene on chromosome 21 is most frequently inactivated in human leukemias. In addition, an increased dose of *RUNX1* is suggested as a basis for several kinds of leukemias. Amplifications of chromosome 21 or the *RUNX1* gene are shown to be associated with leukemias with lymphoid lineage, whereas its involvement in myeloid lineage remains unclear. In this study, we generated *GATA-1* promoter-driven *Runx1* transgenic (Tg) mice, which showed a transient mild increase of megakaryocyte marker-positive myeloid cells but no spontaneous leukemia. These mice were then crossed with BXH2 mice, which have a replication-competent retrovirus in the mouse and develop myeloid leukemia due to insertional mutagenesis by random integration of the virus. Overexpressed *Runx1* transgene in BXH2 mice resulted in shortening of the latency of leukemia with increased frequency of megakaryoblastic leukemia, suggesting that increased *Runx1* dosage is leukemogenic in myeloid lineage. Identifications of retroviral integration sites revealed the genetic alterations that may cooperate with *Runx1* overdose in myeloid leukemogenesis. This mouse model may be useful for analysing the pathogenesis of myeloid leukemias with *RUNX1* overdose, especially to examine whether an extra-copy of *RUNX1* by trisomy 21 is causally related to Down's syndrome-related acute megakaryoblastic leukemia (DS-AMKL).

Oncogene (2005) **24,** 4477–4485. doi:10.1038/sj.onc.1208675
Published online 25 April 2005

Keywords: Runx; GATA-1; CBF; down syndrome; megakaryoblastic leukemia

Introduction

The *RUNX1/AML1* gene encodes the α subunit of PEBP2/CBF, the Runt domain transcription factor that is essential for definitive hematopoiesis and is the most frequently altered gene associated with human leukemia (Look, 1997; Speck and Gilliland, 2002). Haploinsufficiency of *RUNX1* causes familial platelet disorder that is associated with a predisposition to developing acute myeloid leukemia (FPD/AML, OMIM 601399) (Song *et al*., 1999). This implies that the physiological function of *RUNX1* is sensitive to the dosage of the gene. Therefore, it is interesting to note that amplifications of chromosome 21 or *RUNX1* on its own are both associated with sporadic leukemias with lymphoid lineage and occasionally with myeloid lineage (Niini *et al*., 2000). Recent studies employing retrovirus insertional mutagenesis showed that integration into the promoter region of *Runx1* results in overexpression of the gene and induces murine T-cell lymphomas (Wotton *et al*., 2002). In addition, an extra copy of *RUNX1* on chromosome 21 has been suspected to be responsible for the increased risk for Down's syndrome (DS) children to develop leukemia, since the minimum region on chromosome 21 that causes DS contains the *RUNX1* locus (Dufresne-Zacharia *et al*., 1994; Antonarakis, 1998; Reeves *et al*., 2001; Gurbuxani *et al*., 2004). Infants with DS frequently develop transient abnormal myelopoiesis (TAM) and subsequent acute megakaryoblastic leukemia (AMKL). These observations led us to hypothesize that an increased dose of *RUNX1* plays a role in the development of leukemia in myeloid lineage as well as lymphoid lineage.

In this study, we made transgenic (Tg) mice expressing an extra dose of *Runx1* in hematopoietic cells. Then by using retrovirus mutagenesis method, we introduced random mutations into the mouse genome to see if the presence of an extra-copy of *Runx1* would accelerate the development of myeloid leukemia in mice.

*Correspondence: Y Ito, Institute of Molecular and Cell Biology, 61 Biopolis Drive, Proteos, Singapore 138673, Singapore;
E-mail: itoy@imcb.a-star.edu.sg
[6]These two authors contributed equally to this study
Received 15 December 2004; revised 24 February 2005; accepted 3 March 2005; published online 25 April 2005

Results

GATA-1 *promoter-driven* Runx1 *Tg mice showed a transient mild increase of CD61-positive cells but no spontaneous leukemia*

To test the hypothesis that an increased dose of *RUNX1* is responsible for the hematopoietic abnormalities, we generated Tg mice that express mouse *Runx1* under the control of the hematopoietic regulatory domain (HRD) of *GATA-1* (*Runx1* Tg) (Onodera *et al*., 1997). We used the *GATA-1* HRD promoter because GATA-1 is a key transcription factor in the differentiation of both erythrocytes and megakaryocytes (Shivdasani *et al*., 1997), which are two sublineages in a fraction of myeloid lineage cells, and mutations in this gene are associated with DS-AMKL, one of the intriguing case where an increased dose of *RUNX1* is possibly implicated in leukemogenesis (Wechsler *et al*., 2002; Gurbuxani *et al*., 2004). RT–PCR and Western blotting showed that whole bone marrow (BM) cells from *Runx1* Tg mice overexpressed *Runx1* by roughly fivefold above wild-type (WT) mouse level (Figure 1a). We analysed various hematological parameters of neonatal and adult (8-week-old) *Runx1* Tg mice and their WT littermates. No obvious morphological differences were observed but FACS analysis showed increased numbers of cells in the BM and spleen of *Runx1* Tg mice that were positive for the megakaryocyte-specific antigen CD61 (32.3% for Tg versus 25.3% for WT, $P = 0.0004$; Figure 1b). *Runx1* Tg mice also had more leukocytes than WT mice, although these numbers fell within the normal range (Figure 1c). The increased numbers of CD61-positive cells and leukocytes were observed in the neonates but not in the 8-week-old mice. Other hematological analyses, including the megakaryocyte colony-forming assay using adult BM or fetal liver at E14.5, failed to demonstrate an apparent difference between *Runx1* Tg and WT mice. Homozygous *Runx1* Tg mice were also subjected to the same analyses but did not show an augmented phenotype compared to the heterozygotes.

The *Runx1* Tg mice did not develop spontaneous leukemia during a 24-month period of observation. This is consistent with the disappearance of the abnormal myelopoiesis in these mice when they reached adulthood.

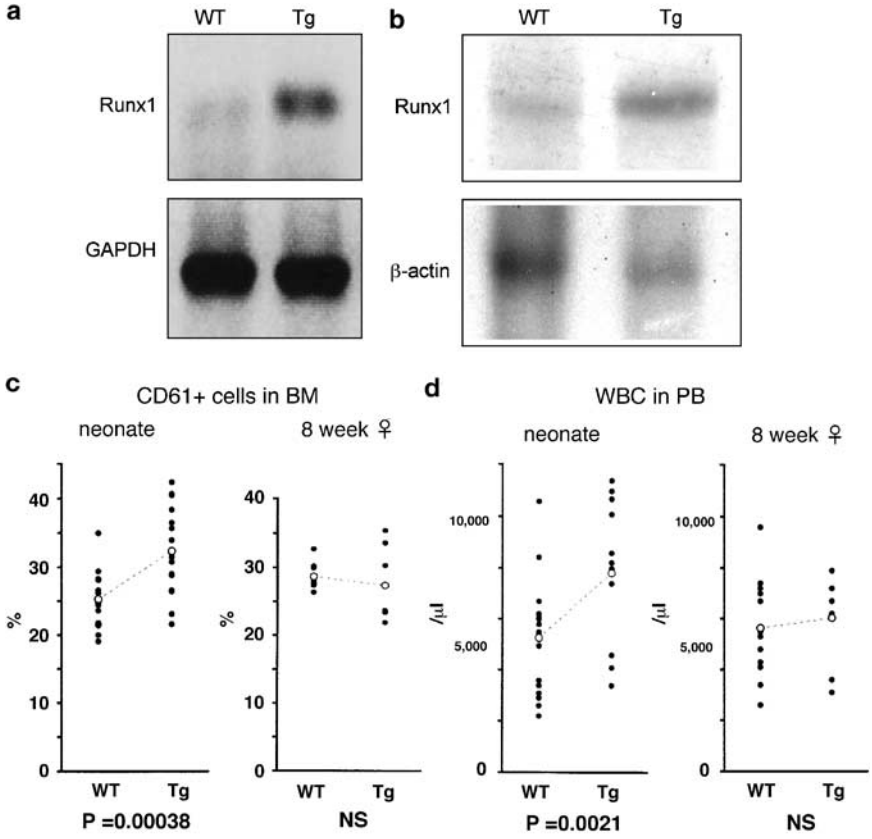

Figure 1 GATA-1 promoter-driven *Runx1* transgenic (Tg) mouse overexpressed *Runx1* by roughly fivefold above wild-type (WT) mouse in their bone marrow (BM) at mRNA (**a**, RT–PCR) and protein (**b**, Western blotting) levels. The expressions of GAPDH and β-actin are shown as internal controls. Neonatal but not adult *Runx1* Tg mice have increased numbers of CD61-positive cells in their BM (**c**) and white blood cells (WBC) in their peripheral blood (PB) (**d**). Only the results of adult females are shown since adult males also did not show these alterations (data not shown). *P*-values, as determined by unpaired Student's *t*-test, are indicated at the bottom. NS, not significant. This experiment involved 16 WT and 17 Runx1 Tg neonates and 13 WT and nine Tg adult females. Each mouse is indicated by a filled circle while the averages of the groups are shown by open circles

BXH2-Runx1 *Tg mice developed CD61-positive myeloid leukemia earlier than BXH2 littermates*

We next tested whether an increased *Runx1* gene dosage would enhance the leukemogenesis. To do this, we crossed the *Runx1* Tg mice with the BXH2 strain, which carries an ecotropic retrovirus that infects neonates through the milk and integrates randomly into the host genomic DNA. This retroviral insertion can lead to either the activation of an oncogene or the disruption of a tumor suppressor gene and, as a consequence, over 90% of the BXH2 mice develop myeloid leukemia at 7–12 months of age (Li *et al*., 1999). The myeloid tropism of the BXH2 mouse is due to its genetic background, and we therefore crossed the *Runx1* Tg mice with the BXH2 strain for a minimum of three generations. The survival of the littermates from 30 BXH2-*Runx1* Tg mice and 41 BXH2 WT mice from generations N3 to N8 was then compared (Figure 2a). This showed that BXH2 *Runx1* Tg mice develop leukemia earlier (mean age of onset: 38.0 versus 45.2 weeks) and show a higher incidence (100 versus ~90% at 14 months) than WT BXH2 mice ($P=0.0067$, Mantel-Cox test). Thus, an overdose of *Runx1* appears to promote leukemogenesis.

FACS analysis showed that two out of eight of the BXH2-*Runx1* Tg leukemias that were analysed exhibited a marked CD61-positive phenotype, unlike any of the 11 leukemias from WT mice ($P=0.0014$, *F*-test, Figure 3a and b). The morphology of the CD61+ leukemic cells showed cytoplasmic blebs that characterize human AMKL (Figure 3c and d). This suggests that an overdose of *Runx1* specifically promotes the development of megakaryoblastic leukemia. All 19 of the leukemic cell samples from the BXH2-*Runx1* Tg and WT mice were positive for the myeloid antigens Gr-1 and Mac-1. They were also occasionally positive for the immature antigen c-kit.

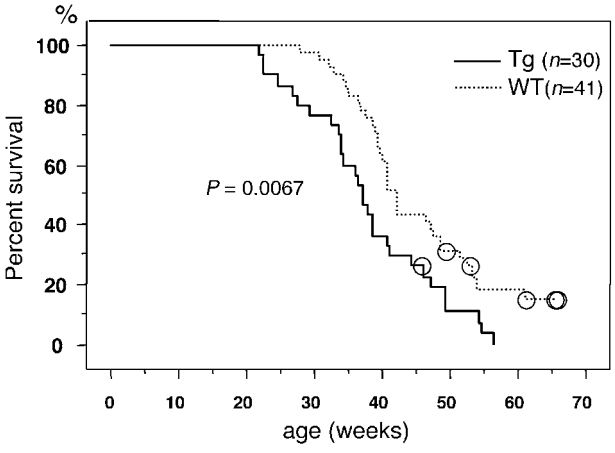

Figure 2 Decreased disease latency in BXH2-*Runx1* Tg mice. The percentage of mice surviving versus age in weeks is plotted for BXH2-*Runx1* Tg mice (solid line, $n=30$) and for their wild-type (WT) littermates (dotted line, $n=41$). Kaplan–Meir method showed significant difference between BXH2-*Runx1* Tg mice and WT controls ($P=0.0067$, Mantel-Cox test). Open circles represent censored cases

Retroviral integration sites revealed the alteration of genes that may cooperate with overdose of Runx1 in myeloid leukemogenesis

To compare the retroviral integration sites (RISs) in the BXH2-*Runx1* Tg and BXH2 WT mice, the genomic DNAs extracted from their leukemic cells were subjected to an inverse PCR method after *Bst*YI digestion (Figure 4). We found 185 integration flanking sequences (tags) in 23 BXH2-*Runx1* Tg mice and 31 BXH2 WT mice (Table 1). These sequences were mapped to the recently assembled mouse genome and the relative locations of the integration sites were compared with 3183 tags from the publicly available retroviral-tagged cancer gene database (RTCGD) (Akagi *et al*., 2004). This comparison revealed that 41 of the integration sites correspond to 26 previously known loci where retroviral integration occurred more than once (common integration site, CIS). These CISs are considered to represent candidate leukemogenic genes. In all, 14 sites overlapped with those that had been described previously to be hit only once. We classified these newly identified loci as RIS-2. In addition, five RISs that have been identified only by our study and hence have been designated as Slis (Singapore leukemia integration site) were classified as RIS-1. The second and third columns from the right in Table 1 show the number of integration events for each RIS in the BXH2 model and in all the models in the RTCGD database (Akagi *et al*., 2004), respectively. The RISs that have been repeatedly identified in the same cancer model are assumed to be more significant candidate genes with regard to the pathogenesis of the specific type of cancer in question.

It is of special interest to note the genes that were hit in the BXH2-*Runx1* Tg mice but not in the BXH2 WT mice, as they may be specifically involved in leukemogenesis of *Runx1* overdose. One of these genes encodes the IL6 receptor β chain, Nki-33 (*IL-6st*/*gp130*), which was hit twice in the BXH2-*Runx1* Tg series but never in the WT BXH2 controls nor in 297 tags from 135 inbred BXH2 mice (see first bolded row in Table 1). IL-6 and its major signaling molecule, STAT3, are known to play an important role in megakaryocyte differentiation (Sui *et al*., 1999; Kirito *et al*., 2002). Thus, *IL6st*/*gp130* is an attractive candidate gene that cooperates with the overdose of *Runx1* to induce megakaryoblastic leukemia.

Individual cases of BXH2 leukemia usually involve 3–5 retroviral integrations that are introduced simultaneously (Li *et al*., 1999). Such concurrently present RISs are summarized in the Interactive Search in the RTCGD database (Akagi *et al*., 2004). Currently, eight Evi-13 (*Runx1*) integration events have been identified. The RISs that coincide with *Runx1* integration events are shown in the far-right column in Table 1. Since *Runx1* is considered to be activated in all eight cases, these concomitantly integrated genes may be candidate genes that cooperate with Runx1 overexpression to induce leukemia. Of these genes, the *c-kit* and *Gfi-1* loci were each hit twice by retroviral integration (see second and fourth highlighted rows by bold in Table 1). c-kit was

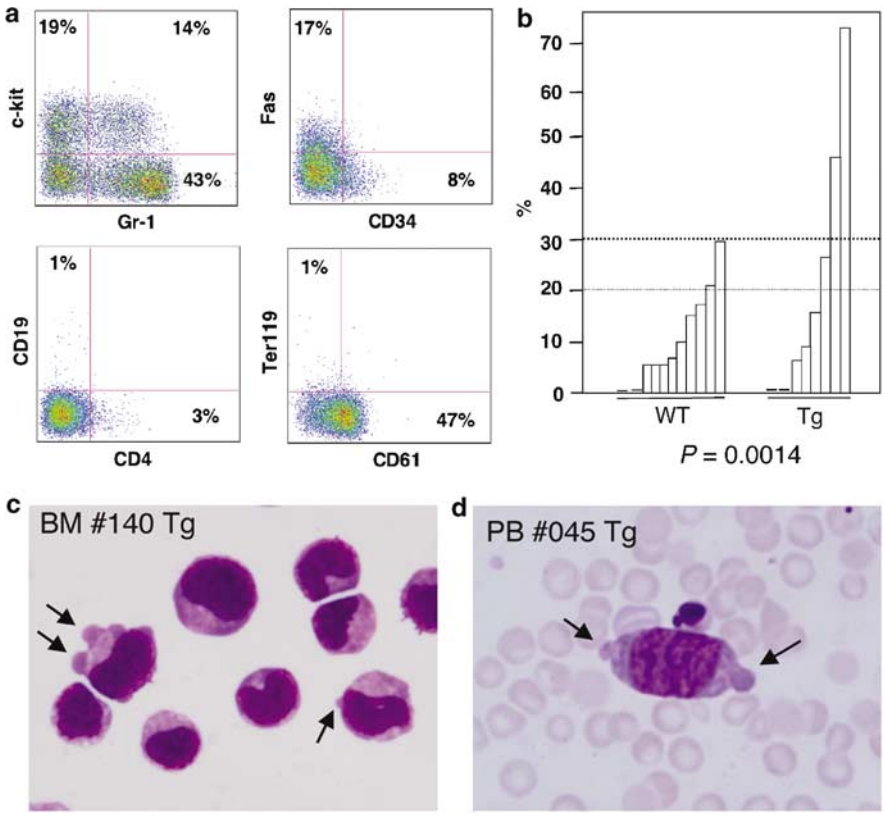

Figure 3 BXH2-*Runx1* Tg mice developed megakaryoblastic leukemia. (**a**) FACS profile of the leukemic cells from a BXH2-*Runx1* Tg mouse #139. (**b**) Percentages of the BM or PB leukemic cells from 11 WT and eight BXH2-*Runx1* Tg mice that are positive for CD61. Each mouse is represented by one bar. Over 30% positivity was considered to indicate a strongly positive sample. Two of the eight BXH2-*Runx1* Tg mice were strongly positive compared to none of the 11 WT controls. This was statistically significant as determined by an *F*-test ($P = 0.0014$). (**c, d**) The morphology of May-Giemsa-stained CD61-positive BXH2 Tg leukemias. The cells are magnified by $\times 1000$. The tissue, the identification number of the mouse and its genotype are indicated in each panel. These leukemic cells show cytoplasmic blebs (arrow) that characterize megakryoblastic leukemia

also hit once in a BXH2-*Runx1* Tg mouse but not in WT littermates. Gfi-1, however, has not been hit in BXH2-*Runx1* Tg mice. Nevertheless, the fact that it has been repeatedly hit together with *Runx1* in other systems makes it a good candidate gene that may cooperate with *Runx1* overdose. The *Ccnd3* locus, which was affected once in a BXH2-*Runx1* Tg mouse, was also hit once along with an integration event into *Runx1* (see third row in bold in Table 1).

To determine whether the leukemic clone with a particular integration site is a major or a minor clone in the mouse, Southern blotting was performed. The result indicated the leukemic cells of #292 mouse carrying c-kit integration was a major clone (Figure 4c): that is, not the minor clone amplified by IPCR, which would not be visible in Southern blotting, suggesting that c-kit integration in this mouse is not a random event and likely to provide growth advantage to the cells.

To verify the implication of the candidate cooperative genes mentioned above and summarized in Figure 5a, we cloned human cyclin D3 promoter spanning -14 to -1014 bp relative to the ATG codon at $+1$ containing three putative Runx binding sites and three putative STAT binding sites (Brooks *et al*., 1996) in front of the luciferase gene and carried out a reporter assay. The cotransfection of RUNX1/PEBP2β and STAT3 into HL60 myeloid leukemia cells revealed more than twofold higher activation compared to that of RUNX1/PEBP2β alone (Figure 5b, lane 6 versus lane 3) and the synergy was completely lost by introduction of a point mutation in the DNA-binding domain of either gene, R174Q in RUNX1 (Michaud *et al*., 2002) or R414A, R417A in STAT3 (Fagerlund *et al*., 2002) (lanes 7 and 8, respectively). This result showed the synergistic activation of cyclinD3 promoter by RUNX1 and STAT3 in a DNA-binding dependent manner.

Discussion

To test the hypothesis that an increased dose of *RUNX1* is leukemogenic in myeloid lineage, we generated *GATA-1* promoter-driven *Runx1* Tg mice, which developed a transient mild increase of megakaryocyte marker CD61 antigen-positive myeloid cells but no spontaneous leukemia. These mice were subsequently crossed with myeloid leukemia-prone BXH2 mice to introduce mutations by retroviral insertional mutagenesis. In

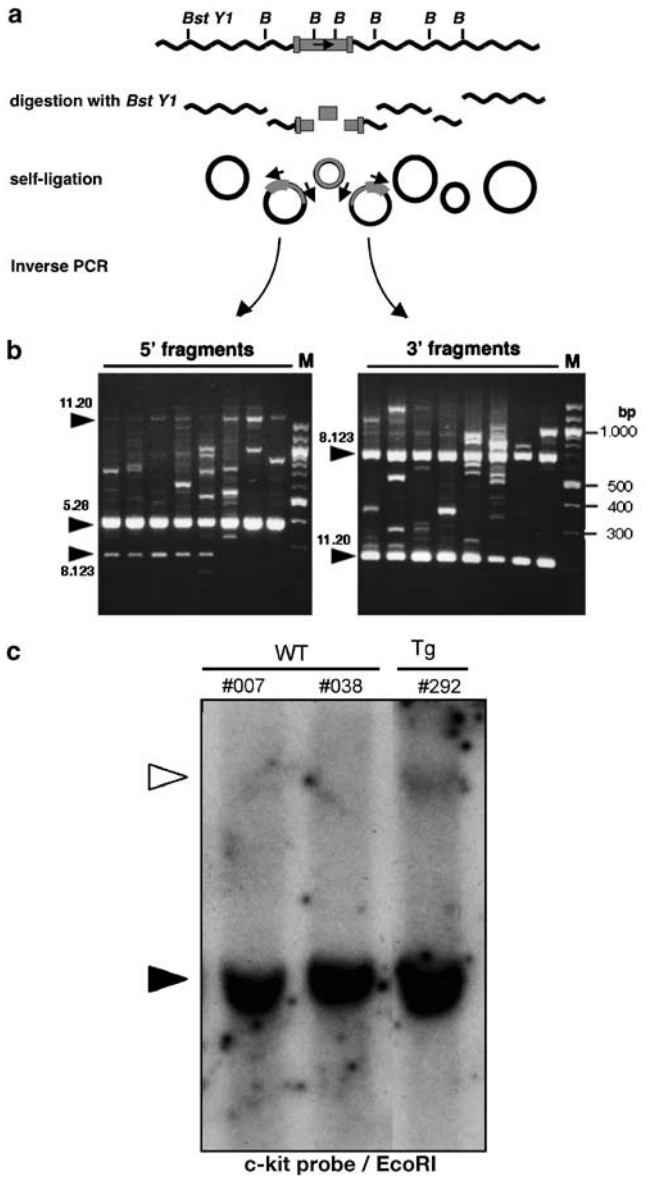

Figure 4 Representative results of the inverse PCR performed on leukemic cells obtained from BXH2-*Runx1* Tg and BXH2 WT mice. (**a**) Schematic depiction of the inverse PCR method. Integration flanking sequences digested by *Bst*YI were self-ligated and amplified separately from 5′-fragments and 3′-fragments. (**b**) Electrophoresis of the IPCR products. Each lane represents individual BXH2 leukemia. The arrowheads depict the germ line-derived bands and are labeled with their corresponding locations on the mouse chromosome (chromosome number followed by a dot and then the position in megabases). Several additional bands were amplified from the somatically acquired integrations in each leukemic cell sample. M denotes the 100 bp DNA ladder that serves as the molecular marker. (**c**) Southern blot hybridization with the c-kit 292 probe. The closed arrowhead depicts a germ line band while the open arrowhead depicts a rearranged band. In all, 10 μg of genomic DNA from the spleen of leukemic mice indicated at the top with genotype are digested with *Eco*RI

effect, we introduced an extra-copy of *Runx1* into BXH2 mouse. The presence of an extra-copy of *Runx1* in BXH2 mice shortened the time required for the onset of leukemia development. The increased dose of *RUNX1* is implicated in lymphoid malignancy to some extent. However, its implication in myeloid malignancy remains unclear. Therefore, to our knowledge, the results presented in this paper are the first evidence that suggests that an overdose of *RUNX1* promotes myeloid leukemogenesis.

Identifications of retroviral integration sites revealed the candidate genetic alterations cooperating with *Runx1* overdose to induce leukemia. The results further support the correlation between *RUNX1* overdose and myeloid leukemia since substantial number of candidate genes highlighted in bold in Table1 and summarized in Figure 5a are known to be involved in myelo/megakaryocyte differentiation. First, *c-Kit* and *IL-6st/gp130* could promote proliferation of myeloid cells by activating STAT3. Both WT IL6st/gp130 and a mutant form of c-Kit that occurs frequently in human myeloid leukemias activate the function of STAT3 (Sui *et al*., 1999; Ning *et al*., 2001). *Gfi-1* may have a similar effect since the overexpression of *Gfi-1* also results in STAT3 activation because it represses the inhibitory effect of PIAS3 (Rodel *et al*., 2000). *Gfi-1* is also shown to be involved in myeloid differentiation (Hock *et al*., 2003) and a member of its gene family, *Gfi-1b*, is essential for the development of megakaryocytes (Saleque *et al*., 2002). Thus, the overexpression of *Gfi-1* may block megakaryocyte differentiation. The aberrant activation of STAT3 together with the overexpression of *Runx1* may lead to dysregulation of *cyclin D1* or *cyclin D3*, since both *STAT3* and *RUNX1* binding sites are located on the regulatory element of *cyclin D1* and *cyclin D3* (Bromberg *et al*., 1999; Strom *et al*., 2000). In fact, we observed a synergy between *RUNX1* and *STAT3* on the regulation of *cyclin D3* promoter (Figure 5b). Enhanced expression of *cyclin D3* might further lead to deregulation of megakaryocyte differentiation since the *cyclin D3* Tg mice showed such defects (Zimmet *et al*., 1997). Therefore, gain-of-function mutations in the *IL-6st/gp130*, *c-kit* and *Gfi-1*, together with overdose of *Runx1* may stimulate the growth of the cell by activating the G1 cyclin through STAT3. This highly speculative model, however, requires further investigation.

The implication of the relationship between *RUNX1* overdose and myeloid malignancy seems most relevant to DS-AMKL, since BXH2-*Runx1* Tg mice frequently developed megakaryoblastic leukemias. The transient mild increase of CD61 antigen-positive myeloid cells in *Runx1* Tg mice also reminds us of TAM, a preleukemic phase preceding AMKL in DS infants. However, previous studies have failed to show clearly that DS-AMKL patients have an elevated expression of *RUNX1* (Gjertson *et al*., 1999; Tassone *et al*., 1999; McElwaine *et al*., 2004). Likewise, in the leukemic cells from BXH2-*Runx1* Tg series, we were unable to detect overexpression of Runx1 (data not shown) although bone marrow from simple *Runx1* Tg mice showed prominent overexpression (Figure 1a). It is possible that overexpression of *Runx1* is necessary at very early stage, probably prior to TAM, for the eventual development of DS-AMKL and it is no longer required at its final full-blown leukemic stage.

Table 1 Classification of RISs identified in leukemic BXH2-*Runx1* Tg and BXH2 WT mice by inverse PCR

Classification of the RISs found in this study	*Genomic position*[a]	*RIS/gene*[b]	*Hits in this study*		*Hits in RTCGD*		*Hits interacting with Runx1*
			Tg	*WT*	*BXH2*	*All*	
Known CIS (26)[c]	11.79	Nf-1 (Evi-2)	2	4	9	14	0
	6.52	HoxA7, A9	3	0	9	13	0
	11.18	Meis1	1	0	10	15	0
	13.28	Evi-15,16(Sox4)	0	1	9	63	0
	10.20	Ahi/Myb	2	3	6	46	2
	13.109	**Nki-33 (Il6st/gp130)**	**2**	**0**	**0**	**2**	**0**
	2.103	Lmo2	1	0	0	2	0
	2.170	Evi-49(BCAS1)	1	1	0	2	0
	4.44	Nki-9(D4Wsu132e)	1	0	0	2	0
	4.133	Runx3	1	1	0	5	0
	5.74	**c-kit/Kdr**	**1**	**0**	**0**	**9**	**2**
	16.78	D16Ertd472e/Btg3	1	0	0	2	0
	17.45	**Evi-14,22(Ccnd3)**	**1**	**0**	**0**	**14**	**1**
	2.35	Nki-2(Ggta1)	0	1	0	2	0
	2.90	sfpi1(Pu.1)	0	1	0	2	0
	2.167	Nki-4(Ptpn1/Cebpb)	0	1	0	17	0
	3.95	Nki-6(Lass2)	0	1	0	2	0
	5.105	**Gfi-1**	0	**1**	1	**63**	**2**
	7.67	Evi-167(Sema4b)	0	1	0	4	0
	7.132	Fgf3	0	1	0	12	0
	10.79	Evi-103(Ptbp1)	0	1	0	4	0
	11.24	Evi-9 (Bcl11A)	0	1	1	7	0
	11.98	Ccr7(Si7)	0	1	0	3	0
	12.79	Lvis4	0	2	1	3	0
	17.30	Cryaa	0	1	0	2	0
	19.31	Casvis-11(Tmem23)	0	1	0	3	0
RIS-1 (5)[c]	Un	Slis-1	1	2	0	0	0
	14.43	Slis-2	1	0 (1)[d]	0	0	0
	16.94	Slis-3	1	0 (2)[d]	0	0	0
	Un	Slis-4	1	2	0	0	0
	14.32	Slis-5	0	1 (1)[d]	0	0	0
RIS-2 (20)[c]	1.87	Akp3	1	0	0	1	0
	2.144	Hars2	1	0	0	1	0
	5.122	BC003324	1	0	0	1	0
	10.24	Arg1	1	0	0	1	0
	12.64	Fv1	1	0	0	1	0
	13.79	Cryba4	1	0	0	2	0
	2.35	Rab14	0	1	0	1	0
	2.164	Zswim3	0	1	0	1	0
	2.168	Stau1	0	1	1	1	0
	2.180	Slco4a1	0	1	0	1	0
	3.89	Arhgef2	0	1	1	1	0
	3.154	Asb17	0	1	0	1	0
	5.62	Tbcld1	0	1	0	1	0
	5.103	E430036I04Rik	0	1	0	1	0
	5.133	A730041O15Rik	0	1	1	2	0
	7.19	Tyrobp	0	1	0	1	0
	9.103	B130017P16Rik	0	1	0	2	0
	9.110	Ngp	0	1	0	1	0
	15.75	Ly6e	0	1	0	1	0
	19.56	Ablim1	0	1	0	1	0
Single RIS (115)[c]	—	—	47	68	0	0	0
Total (166 RISs) 185 tags			74	111	297	3183	60
Number of mice analysed			23	31	135	948	8

[a]The genomic positions of the RISs were determined according to BLAT searching of the UCSC Genome Bioinformatics database. The chromosome number is followed by a dot and then the position in megabases. [b]RISs or candidate genes in the vicinity of the RISs are shown. The underlined gene/RIS represents those whose coding sequence is disrupted. [c]The total numbers of CISs or RISs in each category are indicated in parentheses. [d]Other integrations into Slis were identified in another study of ours that used BXH2 mice with other Runx1 abnormality, Runx1+/− (Yamashita *et al*., described elsewhere). The numbers of each integration event are shown in parenthesis. The bolded rows indicate the particularly interesting RISs that are discussed in the text. Abbreviations: RTCGD, retroviral-tagged cancer gene database; Tg, BHX2 Runx1 transgenic mice; WT, wild-type BXH2 littermate control; CIS, common integration site; RIS, retroviral integration site

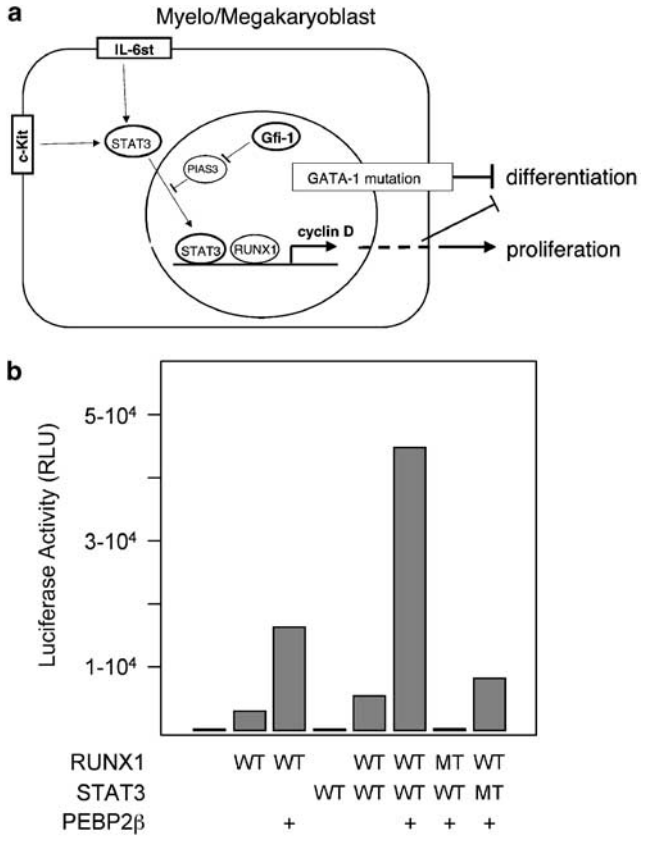

Figure 5 (**a**) Putative relationship between the genes that may cooperate with Runx1 overexpression to induce leukemia. The activation of *IL-6st*, *c-Kit*, and *Gfi-1* by retroviral integration may activate cyclin D through the STAT3 cascade and thereby stimulate the cell to proliferate. This could be enhanced by the overexpression of RUNX1, which could stimulate *cyclin D* expression through its interaction with STAT3. This growth advantage, when partnered with a *GATA1* mutation that blocks differentiation, may drive myelo/megakaryoblasts to become leukemic cells. (**b**) Transactivation of cyclin D3 promoter by both RUNX1 and STAT3 in the presence of IL-6. Wild type (WT) or mutant (MT) form of RUNX1 or STAT3 were cotransfected into HL60 cells with/without PEBP2β in the indicated combinations. The synergistic activation is lost in a DNA-binding mutant of either RUNX1 or STAT3

BXH2-*Runx1* Tg mouse, however, does not fully recapitulate TAM and DS-AMKL. First, the expression level of *Runx1* transgene is roughly fivefold above the WT mouse level, but not 1.5-fold like in trisomy 21. In addition, the phenotypes in the mice seem much milder than those of TAM and DS-AMKL. For example, the leukocyte counts from *Runx1* Tg mice fell within the normal range and no increase of immature myeloid cells was observed at neonates. This phenomenon is significantly different from TAM. Furthermore, not all BXH2-*Runx1* Tg mice develop megakaryoblastic leukemia. Finally, we failed to show that leukemogenesis is associated with the integration of retrovirus into GATA-1 locus in the mouse system, despite the fact that point mutations of GATA-1 are almost obligatorily associated with DS-AMKL. This may be because the chromatin structure around the GATA-1 locus is not favorable for retroviral integration. In support of this possibility, retrovirus integration into the GATA-1 locus has not been observed in all 3183 tags in the RTCGD. Alternatively, the introduction of the Runx1 transgene may have created an artificial situation that mimics that of the absence of GATA-1 function, since GATA-1 itself could be tethered by the excessive expression of Runx1, since Runx1 interacts physically with GATA-1 (Elagib *et al*., 2003). Thus, an excess of the Runx1 protein may lead to a lack of GATA-1 function that substitute for the GATA-1 mutations. If retrovirus integration does not occur on the GATA-1 locus for whatever the reasons, point mutations could have occurred but we failed to observe such mutations either. GATA-1 expressions in BXH2-*Runx1* Tg leukemias were not suppressed compared to those in BXH2 WT leukemias, suggesting that deletion or silencing of *GATA-1* gene did not occur in BXH2-*Runx1* Tg leuekemic cells. A possible explanation for the lack of mutations, deletions, or silencing in GATA-1 is that autoregulation of GATA-1 (Kobayashi *et al*., 2001) may lead to the suppression of the *Runx1* transgene when GATA-1 is impaired. Further investigation is required to determine which of these possibilities are responsible.

Why is overexpresison of *RUNX1* also leukemogenic, despite ample evidence to date showing that loss-of-function of *RUNX1* is a basis for leukemogenesis? One hypothesis is that *RUNX1* should be downregulated at a certain stage in a specific lineage, such as megakaryocyte, to induce a terminal differentiation. Megakaryocyte is known to be regulated strictly by the precise control mechanism governing a number of factors related to cell cycle, mitosis and cytokinesis (Zimmet and Ravid, 2000; Zhang *et al*., 2004). Insufficient downregulation of *RUNX1* due to the increased dose at a certain stage of megakaryocyte differentiation may result in disturbed regulation of cell proliferation and could eventually give rise to TAM, then leukemia. Consistent with this notion, Runx2 Tg mice which overexpress *Runx2* also showed impaired differentiation of T-cell or bone development (Vaillant *et al*., 1999; Liu *et al*., 2001). On the other hand, another mechanism, a constitutive expression of *RUNX1* that may be caused by an increased dose should be considered carefully, since *RUNX1* is shown to be regulated in a cell-cycle-dependent manner (Bernardin-Fried *et al*., 2004).

By using the Tg approach in combination with random retroviral mutagenesis, we show here for the first time evidence that suggests that an overdose of *RUNX1* is involved in the development of myelomegakaryoblastic leukemia. Although there are significant differences between the DS-AMKL and the phenotype of the BXH2-*Runx1* Tg described here as mentioned above, it is remarkable to observe that the presence of an extra-copy of *Runx1* induces megakaryoblastic leukemia at high frequency in our mouse model. It may be possible to recapitulate complete phenotype of DS-AMKL, if we modify our mouse model based on the discussion described above. Further analysis of the level of expression and presence or absence of mutated state of the genes that were identified here by the BXH2-*Runx1*

Tg system (e.g. *IL6st*/*gp130*, *c-Kit*, *Gfi-1*, *cyclin D1*/*3* and *STAT3*) in human leukemia samples will validate the usefulness of this system.

Materials and methods

Construction of the GATA-1 HRD–Runx 1 *Tg mouse*

The Tg mouse that overexpresses mouse *Runx1* under the control of the HRD of *GATA-1* (*Runx1* Tg) was generated by Yokomizo *et al*. and described elsewhere. *Runx1* Tg mice were maintained on the C57BL/6 background. The expression level of Runx1 was investigated in adult bone marrows of the mice by RT–PCR and Western blotting, using anti-Runx1 monoclonal antibody (clone 3.2.5.7., Active Motif, Carlsbad, CA, USA). All animal experiments were performed according to the Guide for the Use of Experimental Animals in Institute of Molecular and Cell Biology.

Generation of BXH2-Runx1 *Tg mice*

To carry out retroviral insertional mutagenesis, C57BL/6-*Runx1* Tg mice were crossed with BXH2 mice (a gift from Dr Scott Kogan). Since the ecotopic retrovirus in the BXH2 mouse is transmissible through the milk, a male *Runx1* Tg mouse was crossed with female inbred BXH2 mice. The BXH2-*Runx1* Tg mice were subjected to experiments after backcrossing for a minimum of three generations.

Hematological analysis

Since inbred BXH2 mice develop leukemia as early as 7 months of age, BXH2-*Runx1* Tg mice were monitored from the age of 5 months. Complete blood cell counts of peripheral blood (CBC) were obtained weekly by an automatic hematology analyzer running veterinary software (Celltac alpha MEK-6358, Nihon Kohden, Osaka, Japan). When the white blood cell (WBC) count increased beyond 30 000/μl, the mice were carefully observed twice a day. Moribund mice were then killed and subjected to necropsy. Abnormalities in hematopoietic tissues were recorded as follows: enlargement of the thymus, liver, and spleen, and swelling of lymph nodes. Leukemic cells from the peripheral blood, bone marrow and spleen were subjected to May-Giemsa staining. Immunophenotypic analysis was carried out by FACS using a standard method. All antibodies were purchased from Pharmingen (San Diego, CA, USA): anti-mouse c-Kit (2B8), Gr-1 (RB6-8C5), Fas (Jo2), CD34 (RAM34), Mac1 (M1/70), B220 (RA3-6B2), Ter119 (TER-119), CD61 (2C9.G2), CD19 (1D3), and CD4 (H129.19).

The murine megakaryocyte colony-forming assay was carried out using MegaCult-C (Stem Cell Technologies Inc., Vancouver, Canada), in which megakaryocytes are stained by acetylcholinesterase activity for accurate scoring of CFU-Mk.

Identification of retroviral integration sites by inverse PCR

In all, 5 μg of genomic DNA extracted from BXH2 leukemic cells from the spleen was digested by *Bst*YI and self-circularized overnight by T4 DNA ligase (New England Biolabs, Inc., MA, USA) at 16°C. Then, 5′ and 3′ integration flanking fragments were amplified individually by inverse PCR (Figure 3a). The first PCRs were performed with AccuPrime Taq (Invitrogen life technologies, Carlsbad, CA, USA) employing an initial preheating step at 95°C for 5 min followed by 30 cycles of 95°C for 1 min, 60°C (5′ LTR) or 55°C (3′ LTR) for 1 min and 68°C for 3 min. The primers used in the first PCRs were 5′Bst-1R (ccggacgagcccccaaatgaa), 5′Bst-1F (ccgtctctgtctttgtgcgtgtgt), 3′Bst-1R (cctgtgtggtcggcatagaaac), and 3′Bst-1F (cagaaagaggggggaatgaaaga). The second PCRs were performed by rTaq (Promega, Madison, WI, USA) employing an initial preheating step at 95°C for 5 min followed by 35 cycles of 95°C for 1 min, 55°C for 1 min and 68°C for 2 min. The primers used were 5′Bst-2R (ctctctgtacttccttgttctg), 5′Bst-2F (gcctgcgtctgattctgtact), 3′Bst-2R (ggcagcacacaaa cctccctctt), and 3′Bst-2F (gggagggtctcctcagagtgatt). The amplified PCR products were cloned by the TA cloning method using the plasmid pGEM-T vector (Phermingen Co, Madison, WI, USA) and subjected to cycle sequencing (Applied Biosystems, Foster City, CA, USA) using the M13-Reverse primer. The position mapping of the RIS on the mouse chromosome was performed by BLAT searching of the UCSC Genome Bioinformatics database (http://genome.ucsc.edu). The definition of a common integration site (CIS) was the same in the retroviral-tagged cancer gene database (RTCGD) (http://RTCGD.ncifcrf.gov); each window size is 100, 50, or 30 kb for CISs with four (or more), three, or two insertions, respectively, in each model (Akagi *et al*., 2004).

Southern blotting

Southern blotting was performed in a standard procedure using random-primed [^{32}P]dCTP labeling. The genomic DNA probe for c-kit locus is the 486 bp *Bst*YI-*Stu*I fragment in the vicinity of the integration site in leukemia#292.

Transcription assay

The luciferase reporter plasmid pXP2-cyclinD3 promoter-luc and the effecter plasmids, pEF-RUNX1, pEF-PEBP2β, pXJ-STAT3, pXJ-STAT3 (R414A, R417A) were transfected at a fixed ratio into HL60 cells by a nonliposomal transfection reagent, FuGENE6. The transfected cells were incubated for 48 h in the presence of IL-6 stimulation (40 ng/ml) and assayed as previously described (Osato *et al*., 1999).

Acknowledgements
We thank Scott Kogan for his gift of the BXH2 mice and Gwee QiRu, Tan Mia Yan, Melissa Y Lin, and Gregory M Cottles for their technical assistance. This study was supported by A*STAR (Agency for Science, Technology and Research), Singapore.

References

Akagi K, Suzuki T, Stephens RM, Jenkins NA and Copeland NG. (2004). *Nucleic Acids Res.*, **32** (Database issue), D523–D527.

Antonarakis SE. (1998). *Genomics*, **51,** 1–16.

Bernardin-Fried F, Kummalue T, Leijen S, Collector MI, Ravid K and Friedman AD. (2004). *J. Biol. Chem.*, **279,** 15678–15687.

Bromberg JF, Wrzeszczynska MH, Devgan G, Zhao Y, Pestell RG, Albanese C and Darnell Jr JE. (1999). *Cell*, **98,** 295–303.

Brooks AR, Shiffman D, Chan CS, Brooks EE and Milner PG. (1996). *J. Biol. Chem.*, **271,** 9090–9099.

Dufresne-Zacharia MC, Dahmane N, Theophile D, Orti R, Chettouh Z, Sinet PM and Delabar JM. (1994). *Genomics*, **19,** 462–469.

Elagib KE, Racke FK, Mogass M, Khetawat R, Delehanty LL and Goldfarb AN. (2003). *Blood*, **101,** 4333–4341.
Fagerlund R, Melen K, Kinnunen L and Julkunen I. (2002). *J. Biol. Chem.*, **277,** 30072–30078.
Gjertson C, Sturm KS and Berger CN. (1999). *Clin. Immunol.*, **91,** 50–60.
Gurbuxani S, Vyas P and Crispino JD. (2004). *Blood*, **103,** 399–406.
Hock H, Hamblen MJ, Rooke HM, Traver D, Bronson RT, Cameron S and Orkin SH. (2003). *Immunity*, **18,** 109–120.
Kirito K, Osawa M, Morita H, Shimizu R, Yamamoto M, Oda A, Fujita H, Tanaka M, Nakajima K, Miura Y, Ozawa K and Komatsu N. (2002). *Blood*, **99,** 3220–3227.
Kobayashi M, Nishikawa K and Yamamoto M. (2001). *Development*, **128,** 2341–2350.
Li J, Shen H, Himmel KL, Dupuy AJ, Largaespada DA, Nakamura T, Shaughnessy Jr JD, Jenkins NA and Copeland NG. (1999). *Nat. Genet.*, **23,** 348–353.
Liu W, Toyosawa S, Furuichi T, Kanatani N, Yoshida C, Liu Y, Himeno M, Narai S, Yamaguchi A and Komori T. (2001). *J. Cell. Biol.*, **155,** 157–166.
Look AT. (1997). *Science*, **278,** 1059–1064.
McElwaine S, Mulligan C, Groet J, Spinelli M, Rinaldi A, Denyer G, Mensah A, Cavani S, Baldo C, Dagna-Bricarelli F, Hann I, Basso G, Cotter FE and Nizetic D. (2004). *Br. J. Haematol.*, **125,** 729–742.
Michaud J, Wu F, Osato M, Cottles GM, Yanagida M, Asou N, Shigesada K, Ito Y, Benson KF, Raskind WH, Rossier C, Antonarakis SE, Israels S, McNicol A, Weiss H, Horwitz M and Scott HS. (2002). *Blood*, **99,** 1364–1372.
Niini T, Kanerva J, Vettenranta K, Saarinen-Pihkala UM and Knuutila S. (2000). *Haematologica*, **85,** 362–366.
Ning ZQ, Li J and Arceci RJ. (2001). *Blood*, **97,** 3559–3567.
Onodera K, Takahashi S, Nishimura S, Ohta J, Motohashi H, Yomogida K, Hayashi N, Engel JD and Yamamoto M. (1997). *Proc. Natl. Acad. Sci. USA*, **94,** 4487–4492.
Osato M, Asou N, Abdalla E, Hoshino K, Yamasaki H, Okubo T, Suzushima H, Takatsuki K, Kanno T, Shigesada K and Ito Y. (1999). *Blood*, **93,** 1817–1824.
Reeves RH, Baxter LL and Richtsmeier JT. (2001). *Trends Genet.*, **17,** 83–88.
Rodel B, Tavassoli K, Karsunky H, Schmidt T, Bachmann M, Schaper F, Heinrich P, Shuai K, Elsasser HP and Moroy T. (2000). *EMBO J.*, **19,** 5845–5855.
Saleque S, Cameron S and Orkin SH. (2002). *Genes Dev.*, **16,** 301–306.
Shivdasani RA, Fujiwara Y, McDevitt MA and Orkin SH. (1997). *EMBO J.*, **16,** 3965–3973.
Song WJ, Sullivan MG, Legare RD, Hutchings S, Tan X, Kufrin D, Ratajczak J, Resende IC, Haworth C, Hock R, Loh M, Felix C, Roy DC, Busque L, Kurnit D, Willman C, Gewirtz AM, Speck NA, Bushweller JH, Li FP, Gardiner K, Poncz M, Maris JM and Gilliland DG. (1999). *Nat. Genet.*, **23,** 166–175.
Speck NA and Gilliland DG. (2002). *Nat. Rev. Cancer*, **2,** 502–513.
Strom DK, Nip J, Westendorf JJ, Linggi B, Lutterbach B, Downing JR, Lenny N and Hiebert SW. (2000). *J. Biol. Chem.*, **275,** 3438–3445.
Sui X, Tsuji K, Ebihara Y, Tanaka R, Muraoka K, Yoshida M, Yamada K, Yasukawa K, Taga T, Kishimoto T and Nakahata T. (1999). *Blood*, **93,** 2525–2532.
Tassone F, Lucas R, Slavov D, Kavsan V, Crnic L and Gardiner K. (1999). *J. Neural. Transm.*, **57** (Suppl)**,** 179–195.
Vaillant F, Blyth K, Terry A, Bell M, Cameron ER, Neil J and Stewart M. (1999). *Oncogene*, **18,** 7124–7134.
Wechsler J, Greene M, McDevitt MA, Anastasi J, Karp JE, Le Beau MM and Crispino JD. (2002). *Nat. Genet.*, **32,** 148–152.
Wotton S, Stewart M, Blyth K, Vaillant F, Kilbey A, Neil JC and Cameron ER. (2002). *Cancer Res.*, **62,** 7181–7185.
Zhang Y, Nagata Y, Yu G, Nguyen HG, Jones MR, Toselli P, Jackson CW, Tatsuka M, Todokoro K and Ravid K. (2004). *Blood*, **103,** 3717–3726.
Zimmet J and Ravid K. (2000). *Exp. Hematol.*, **28,** 3–16.
Zimmet JM, Ladd D, Jackson CW, Stenberg PE and Ravid K. (1997). *Mol. Cell. Biol.*, **17,** 7248–7259.